

Extractive desulfurization of model fuels with a nitrogen-containing heterocyclic ionic liquid

Guojia Yu, Dongyu Jin, Xinyu Li, Fan Zhang, Shichao Tian, Yixin Qu, Zhiyong Zhou (✉), Zhongqi Ren (✉)

College of Chemical Engineering, Beijing University of Chemical Technology, Beijing 100029, China

© Higher Education Press 2022

Abstract A nitrogen-containing ionic liquid was synthesized using an aromatic nitrogen-containing heterocyclic and an amino acid, and applied to the extractive desulfurization process to remove benzothiophene, dibenzothiophene, and 4,6-dimethyldibenzothiophene from a model fuel oil. Chemical characterizations and simulation using Gaussian 09 software confirmed the rationality of an ionic liquid structure. Classification of non-covalent interactions between the ionic liquid and the three sulfur-containing contaminants was studied by reduced density gradient analysis. The viscosity of the ionic liquid was adjusted by addition of polyethylene glycol. Under extraction conditions of the volume of ionic liquid to oil as 1:1 and temperature as room temperature, the desulfurization selectivity of ionic liquid followed the order of 4,6-dimethyldibenzothiophene (15 min) < benzothiophene (15 min) \approx dibenzothiophene (10 min). Addition of *p*-xylene and cyclohexene to the fuel oil had little effect. The extractant remained stable and effective after multiple regeneration cycles.

Keywords extractive desulfurization, nitrogen-containing heterocyclic ionic liquid, reduced density gradient analysis, desulfurization selectivity

1 Introduction

The removal of organic sulfides from fuel oil remains an urgent issue [1,2]. The presence of certain sulfides can cause equipment corrosion and catalyst poisoning, air pollution, acid rain, and lead to human edema, stomach problems, and even cause central nervous system poisoning in severe cases [3,4]. Sulfides can also accelerate oxidation and deterioration of the oil. Since the

European Union's sulfur content standard was set at 10 ppm (10^{-6}) in 2008 [5], many improvements to the sulfide-removal process have been studied in experimental research and industrial exploration. There are many types of sulfides in oil: mercaptans, thioethers, and disulfides can be removed by hydrodesulfurization; thiophene and its derivatives of five-membered heterocyclic compounds are similar in chemical properties to aromatic hydrocarbons, which are hard to remove by cracking and steric hindrance makes it difficult for the alkyl group to participate in the hydrodesulfurization process [6,7]. Extraction desulfurization (EDS) [8–10] has mild and simple operating conditions, and has also been extensively studied, with significant focus on selection of extractants. Traditional commercially available organic solvents [11,12], such as *N*-formylmorpholine, sulfolane, *N,N*-dimethylformamide, and *N*-methylpyrrolidone, may dissolve in fuel oil, causing fuel pollution, and are environmentally unfriendly.

Ionic liquids (ILs) [13], a new class of green solvents, are molten salts that usually consist of large organic cations in combination with a vast variety of mainly inorganic anions. ILs have been the subject of much research and have become good substitutes for traditional volatile extractants due to their unique physical and chemical properties (non-volatility, high polarity, high chemical and high thermal stability, designability) [14,15]. Conventional quaternary ammonium salts, quaternary phosphonium salts, pyridine or imidazole (Im), pyrrolidone-based cations, and bis(trifluoromethylsulfonyl)imide ($[\text{NTf}_2]^-$), tetrachloroaluminate, tetrafluoroborate ($[\text{BF}_4]^-$), and hexafluorophosphate anions have been widely used in EDS processes [16,17]. For instance, Holbrey et al. [18] found that the EDS efficiency of IL was mainly determined by the type of cation, and there was little direct effect of the anion. The cations were ranked as follows for this application: alkylpyridine \approx pyridine \approx imidazolium pyrrolidone. Butt et al. [19] also verified the positive effect of the cations; anions like

Received December 5, 2021; accepted February 25, 2022

E-mails: zhouzy@mail.buct.edu.cn (Zhou Z.), renzq@mail.buct.edu.cn (Ren Z.)

[NTf₂]⁻ and BF₄⁻ had only minor impact. [NTf₂]⁻-based ILs were more efficient compared with other anions in the desulfurization process [20,21]. Li et al. synthesized a dual IL based on Im and pyridine [22]. Under the best operating conditions (IL/oil mass ratio = 2:1, 30 °C, 30 min), the desulfurization efficiency reached 79.72%. Deep desulfurization was achieved after five cycles. Wang et al. synthesized and characterized several trialkylamine-based ILs [23]. The removal efficiencies of thiophene, benzothiophene (BT), and dibenzothiophene (DBT) from a model oil by tris(3,6-dioxahexyl) ammonium salicylate were 72.68%, 76.31%, and 83.94%, respectively, under the best conditions. Removal efficiency did not decrease significantly after five extraction cycles. Butt et al. [24] found that EDS efficiency varied with *N*-ethylene glycol chain length and *N*-allyl or *N*-benzyl substitution on imidazolium ILs. ¹H NMR confirmed that π - π interaction between the benzimidazolium ions and DBT played a major role in the high efficiency.

Our team also synthesized two ILs by proton-exchange reaction between 1,8-diazabicyclo[5.4.0]undec-7-ene (DBU), 1,1,3,3-tetramethylguanidine (TMG), and Im [25]. These two ILs exhibited removal efficiencies of 79.2% and 69.4%, 68.4% and 57.7%, and 61.2% and 54.4% for DBT, 4,6-dimethyldibenzothiophene (DMDBT), and BT, respectively. Relatively speaking, since the anions are completely the same, it is preliminarily believed that the *N*-containing heterocyclic structure is the main contribution to the improvement of the extraction efficiency. Based on this, we then synthesized a series of different nitrogen-containing heterocyclic ILs to study the influence of different heterocyclic structures [26], which exhibited removal efficiencies for organic sulfur as follows: DBU (82.55%) > *N*-formylmorpholine (61.03%) > 1-hexyl-3-methylimidazolium (43.95%) > *N*-methylmorpholine (32.95%). These DBU-based ILs showed good interaction with thiophene sulfides. Nashef et al. combined pyrrolium and phosphonium-based ILs with specific molecular compounds (Im, polyethylene glycol (PEG) 200, and sulfolane) [27]. PEG 200 and sulfolane were observed to have more positive effects on performance of the IL than Im. Wang et al. found that when the volume ratio of PEG200 to DBT was 0.7:5, PEG 200 had a certain extraction capacity for DBT at 60 °C for 5 h [28]. Therefore, while adjusting the viscosity, it can promote the extraction process. Also, it completely immiscible with oil phase is a major advantage over sulfolane.

Herein, [L-pyroglutamic acid] ([L-Pyro]), which also contains a nitrogen-containing heterocyclic ring, is used for the protonation process. [DBU][L-Pyro] was synthesized and treated with PEG 200 as a phase regulator. Serial characterizations and quantum chemical calculations were used to explore the formation of [DBU][L-Pyro] and its interaction with thiophene sulfides at the

molecular level. The influences of factors such as extraction time, extractant/oil volume ratio, and competition between olefins and aromatics were also studied.

2 Experimental

2.1 Chemicals

DBU (99%) was purchased from Shanghai Aladdin Biochemical Technology Co., Ltd. L-Pyro (98%) was purchased from Shanghai Macklin Biochemical Co., Ltd. PEG200, methanol, *n*-octane, and tetradecane were supplied by Sinopharm Chemical Reagent Co., Ltd. BT, DBT, and DMDBT were obtained from Adamas Reagent Co., Ltd. All chemicals were of analytical grade and used directly without further pretreatment.

2.2 Preparation of ILs

DBU (0.01 mol) and L-Pyro (0.01 mol) were added to a round-bottom flask with 50 mL anhydrous methanol and stirred at room temperature for 24 h, [DBU][L-Pyro] IL with higher viscosity was obtained by removing the methanol by rotary evaporation and a vacuum drying oven. The synthesis pathway is shown in Fig. 1. A specified molar ratio of PEG200 was then added and the mixture agitated at 60 °C for 3 h to achieve [DBU][L-Pyro][PEG200], also labelled as [IL][PEG200].

2.3 Extraction experiments

Model oil with an initial concentration of 500 ppm was prepared by dissolving the sulfur compounds (DBT, BT, DMDBT) in tetradecane. The prepared ILs and model oil (v:v = 1:1) were added to a 10 mL glass sample bottle, fully stirred at room temperature and allowed to stand for 30 min after reaction. The supernatant was obtained by

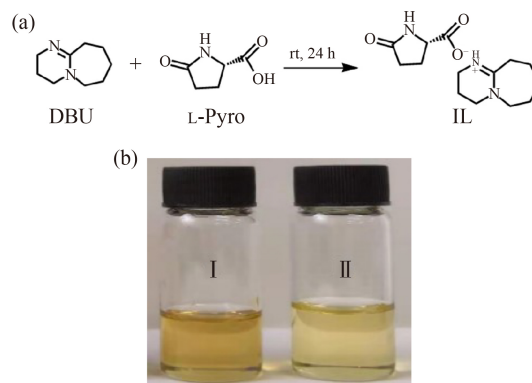


Fig. 1 (a) Synthetic pathway of [DBU][L-Pyro] and (b) appearance of (I) [DBU][L-Pyro] and (II) [IL][PEG200].

filtering with an organic-phase filter (0.45 μm), and analyzed by gas chromatography using *n*-octane as the internal standard. The extraction efficiency was calculated according to the following formula:

$$\text{Extraction efficiency (\%)} = (C_1 - C_2) \times \frac{100}{C_1}, \quad (1)$$

where C_1 (ppm) and C_2 (ppm) were the initial and final concentrations of sulfur in model oil, respectively.

2.4 Characterization

The structures of the prepared ILs were characterized by Fourier transform infrared (FTIR) spectroscopy (Thermo Electron, NEXUS8700, USA) and ^1H nuclear magnetic resonance (^1H NMR) spectroscopy (Bruker AV400MHz, Germany), using dimethyl sulfoxide- d_6 or CDCl_3 as a solvent. The FTIR and ^1H NMR spectra of the reactants and ILs are shown in Figs. S1 and S2 (cf. Electronic Supplementary Material, ESM).

2.5 Simulation calculation

Since the determination of the IL structure by characterization alone was insufficient, the optimization of IL structure was performed at the M06-2X/6-31++G(d,p) level of the density functional theory using Gaussian 09 software [29]. All the structural optimizations were free of negative frequencies. The frequency values at the optimal IL configuration were chosen for the vibrational spectra with a scaling factor of 0.979 [30]. The interaction between the IL/tetradecane and sulfides was also studied with the same basis set, where several different initial geometries of IL and sulfides were optimized to ensure the optimal configuration. The calculation equation was according to formula (2):

$$\Delta E = E_{\text{IL}} - (E_{\text{IL}} + E_{\text{S}}) + E_{\text{BSSE}}, \quad (2)$$

where S represents BT, DBT or DMDBT. The “energy” (ΔE) was determined using the difference between the total energy values of the IL and constituent components, and Basis-set superposition error (BSSE) was considered.

Meanwhile, the interaction forces were analyzed by reduced density gradient analysis to visualize and categorize the non-covalent interactions [31,32].

2.6 Detection and analysis methods

The upper oil phase was collected as the sample, diluted, and injected into a gas chromatograph (GC-2014C, HP-5 column: 30 m \times 0.32 mm \times 0.25 mm). The internal standard method was used to determine the sulfide content. The measurements were repeated three times to determine the experimental accuracy. Viscosities of the ILs were measured at 298 K using a Thermo Fisher rotational rheometer (HAAKE Mars 40, Germany).

3 Results and discussion

3.1 Desulfurization performance of [DBU][L-Pyro] IL

The desulfurization performance of [DBU][L-Pyro] is presented in Table 1. [DBU][L-Pyro] showed extraction efficiencies for BT, DBT, and DMDBT of 64.25%, 69.05%, and 30.94%, respectively.

3.2 Simulation calculation of IL

The simulated infrared spectrum was obtained (Fig. 2) by frequency analysis. Table 2 provides the interactions between each substance-related vibration pattern [33]. The difference between the sample amount shown in the experimental spectrum and the number of calculated molecules might result in a shift or intensity change of a molecular vibrational frequency. Nevertheless, the characteristic peaks of the simulated spectrum agreed surprisingly well with the experimental spectra, as shown in Fig. S3 (cf. ESM), giving a correlation coefficient R^2 of 0.9918.

The optimized geometries of DBU, L-Pyro, IL are shown in Fig. 3, and the structures between IL and sulfides are shown in Fig. 3(a). The interaction energies between IL and BT, DBT, and DMDBT were calculated to be -52.56 , -66.33 , and -67.61 $\text{kJ}\cdot\text{mol}^{-1}$, respectively, following the order DMDBT > DBT > BT. This was not in agreement with the experimental data. Conventionally, the extraction process depends on the distribution equilibrium of the sulfides between the IL and the model solvent; therefore, the interaction model between

Table 1 Desulfurization efficiency of [DBU][L-Pyro] IL ^{a)}

| IL-[DBU][L-Pyro] | BT | DBT | DMDBT |
|-------------------------|-------|-------|-------|
| Extraction efficiency/% | 64.25 | 69.05 | 30.94 |

a) Reaction conditions: 50 $^\circ\text{C}$, 30 min, $v_{\text{IL}}:v_{\text{oil}} = 1:1$.

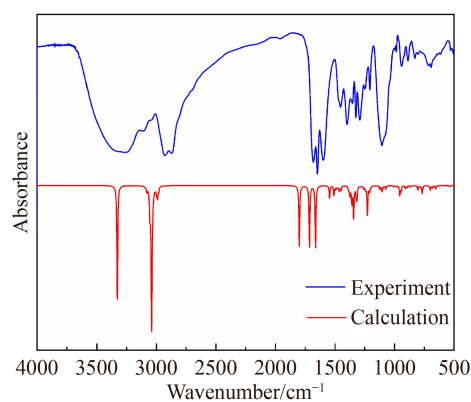
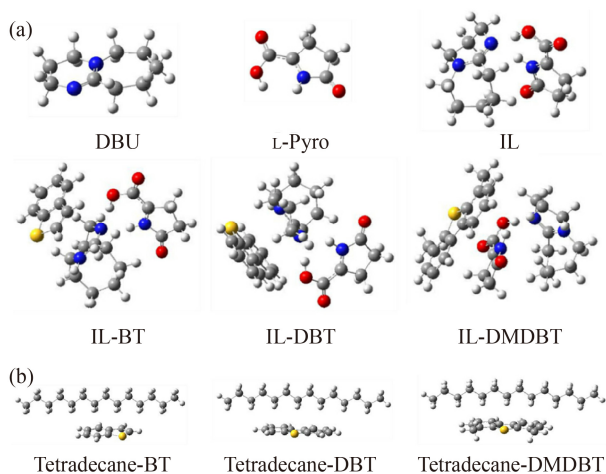


Fig. 2 Comparison between experimental and calculated vibrational spectra determined using the M06-2X/6-31++G(d,p) method for the IL systems.

Table 2 Comparison of experimental and calculated vibrational frequencies at the M06-2X/6-31++G(d,p) level

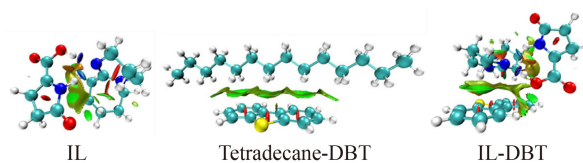
| Bond | Source | Calculation/cm ⁻¹ | Experiment/cm ⁻¹ |
|-----------------------------------|------------------------|------------------------------|-----------------------------|
| –C=N | –C=N in DBU | 1662.8 | 1593.8 |
| –C=O | –C=O in carbonyl group | 1713.6 | 1648.1 |
| –C=O | –C=O in –COOH | 1798.9 | 1680.7 |
| –OH | O–H in –COOH | 3327.3 | 3392.2 |
| –NH | –NH in –NH···C=O | 3041.4 | 3236.2 |
| –CH ₂ –CH ₂ | Six-membered ring | 2989.8 | 2934.1 |
| –CH ₂ –CH ₂ | Seven-membered ring | 3038.5 | 3102.2 |
| –C–N | –C–N in DBU | 1342.7 | 1400.3 |
| –C–N | –C–N in L-Pyro | 1227.1 | 1292.3 |
| –CH | –CH ₂ – | 766.9 | 693.1 |

**Fig. 3** Optimized structures of (a) DBU, L-Pyro, IL, and the IL and (b) tetradecane interacting with BT, DBT, and DMDBT. Color keys: white, hydrogen; grey, carbon; blue, nitrogen; yellow, sulfur; red, oxygen.

tetradecane and sulfides was also explored (Fig. 3(b)). The interaction types could be clearly ascribed to the C–H··· π interaction. The corresponding action energy values were -28.36 , -35.47 , and -49.84 kJ·mol⁻¹, respectively. The comparison showed that the heat of reaction of the two interactions was DBT > BT > DMDBT (-30.86 , -24.2 , and -17.77 kJ·mol⁻¹), which reasonably explained the experimental results. It also could be preliminarily inferred that the aromatic ring might play a positive role in the EDS process, thereby enhancing the interaction between IL and sulfur-containing compounds. For DMDBT, steric hindrance of the methyl group was the main obstacle to extraction [34].

This analysis (Fig. 4) also confirmed the C–H··· π weak interaction between tetradecane and DBT. Interactions between the IL and DBT molecules occurred almost completely in the [DBU]⁺ plane. Herein, the van der Waals force and hydrogen bonding interaction promoted the extractive desulfurization. This might prove our previous conjecture concerning the effective role of the DBU heterocyclic ring from the side.

Considering the high viscosity of [DBU][L-Pyro] IL

**Fig. 4** Gradient isosurfaces ($s = 0.5$ au) for the most stable configuration during extractive desulfurization. The surfaces are colored on a red–green–blue scale according to values of $\sin(\lambda)\rho$, ranging from -0.035 to 0.02 au. Red areas indicate strong attractive interactions and blue areas indicate strong nonbonded overlap. Color keys: white, hydrogen; blue–green, carbon; blue, nitrogen; yellow, sulfur; red, oxygen.

(6760.8 mPa·s, room temperature), PEG200 was added at different molar ratios (1:2, 1:1, 2:1). The desulfurization efficiencies of [IL][PEG200] (1:1) for BT, DBT, and DMDBT were 67.32%, 70.83%, and 36.16%, respectively, as shown in Table 3. Although this improvement was relatively small, it reduced the reaction temperature. Considering the cost of the IL, the 1:1 volume ratio of IL and PEG200 was selected.

3.3 Optimization of desulfurization process

3.3.1 Effect of extraction time

The desulfurization efficiency was measured for different liquid-liquid extraction times (Fig. 5). Extraction efficiency of the sulfides increased faster during the initial period. The equilibrium extraction efficiencies were 70.82% for DBT, 67.42% for BT, and 36.16% for DMDBT. The standing time after extraction had little effect on the final desulfurization efficiency, which enables shortening of the total extraction process time to a certain extent. The ¹H NMR spectrum of the upper oil phase, shown in Fig. S4 (cf. ESM), indicated that the model oil will not be miscible with [IL][PEG200] and will not cause fuel pollution.

3.3.2 Effect of volume ratio of IL and model oil

The volume ratio between [IL][PEG200] and the model oil is a significant factor affecting the desulfurization process. Figure 6 shows that the slope of the extraction efficiency became steeper with an increase in this ratio from 1:5 to 1:1 and became gentler after 1:1. When the ratio was 3:1, the extraction efficiencies of BT, DBT, and

Table 3 Desulfurization efficiency of IL with different molar ratios of PEG200^{a)}

| ILs | Molar ratio | S-removal efficiency/% | | |
|--------------|-------------|------------------------|-------|-------|
| | | BT | DBT | DMDBT |
| [IL][PEG200] | 1:2 | 65.55 | 67.82 | 31.55 |
| | 1:1 | 67.32 | 70.83 | 36.16 |
| | 2:1 | 67.15 | 70.31 | 35.22 |

a) Reaction conditions: room temperature, 30 min, $v_{[IL][PEG200]}:v_{oil} = 1:1$.

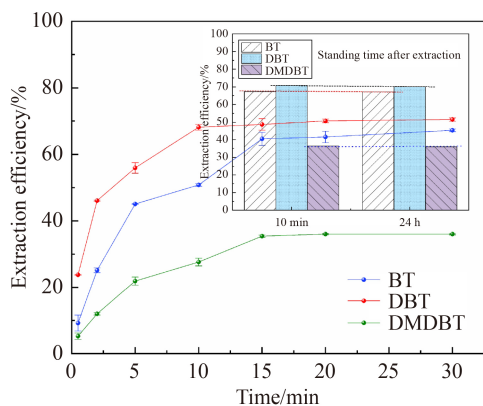


Fig. 5 Effect of extraction time on sulfur removal by [IL][PEG200].

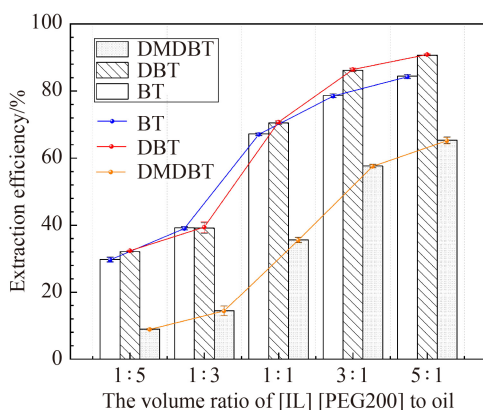


Fig. 6 Effect of volume ratio of [IL][PEG200] to oil on sulfide extraction efficiency.

DMDBT were 78.66%, 86.48%, and 58.01%, respectively. Considering the economic cost, the 1:1 ratio was selected for subsequent experiments.

3.3.3 Multiple cycle extraction

Generally, the desulfurization efficiency of a single extraction cannot meet the requirements for deep desulfurization (< 10 ppm), multi-stage extraction was used to achieve high-efficiency desulfurization, as shown in Fig. 7. Desulfurization of BT and DBT was largely achieved after four cycles, with BT at 2.84 ppm and DBT at 6.75 ppm. The DMDBT content reached 8.15 ppm after 11 cycles, mainly due to the minimal further drop in DMDBT in each step at low concentrations. In summary, [IL][PEG200] was feasible as an extractant to remove BT, DBT, and DMDBT from a model oil.

3.3.4 Effect of olefins and aromatics on desulfurization efficiency

Real gasoline or diesel contains complex mixtures of various hydrocarbons, which may affect desulfurization efficiency. Therefore, 5 and 15 wt% each of *p*-xylene and cyclohexene were chosen as respective

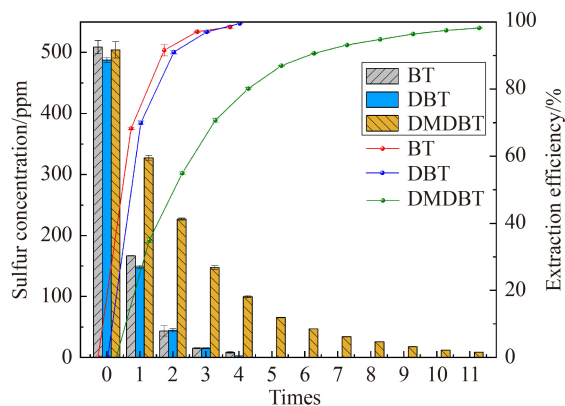


Fig. 7 Sulfur concentration in fuel oil with multiple cycles of extractive desulfurization.

representatives of aromatic and olefin components, and added into the model oil. The results in Fig. 8 indicated that neither *p*-xylene nor cyclohexene influenced the model oil system: reduction of desulfurization efficiency was controlled to within 1%.

3.3.5 Recycling and regeneration

The recovery and regeneration of IL has far-reaching significance for further industrial applications and the development of green chemistry. The studies of recycling and regeneration are shown in Fig. 9. [IL][PEG200] was first directly reused without any special treatment, i.e., after the initial cycle, the upper oil phase was removed by simple decantation and fresh model oil was added to the next cycle under the same extraction conditions. The effect of repeated use is shown in Fig. 9(a): the extraction efficiency for sulfides decreased with increasing number of repeated cycles. The system could no longer extract DMDBT after five repeated cycles and the removal efficiencies of DBT and BT were significantly reduced.

[IL][PEG200] was then extracted and processed three times by cyclohexane, and the residual cyclohexane removed by rotary evaporation under vacuum. The

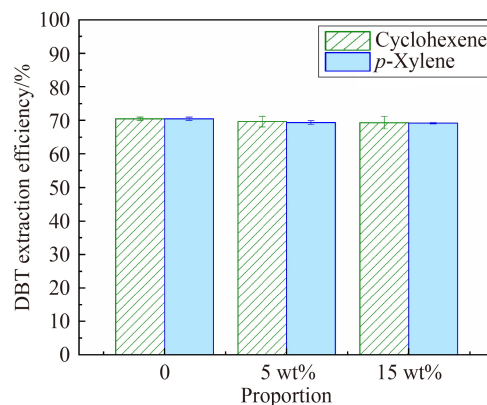


Fig. 8 Effect of olefins and aromatic additions to model fuel on desulfurization efficiency.

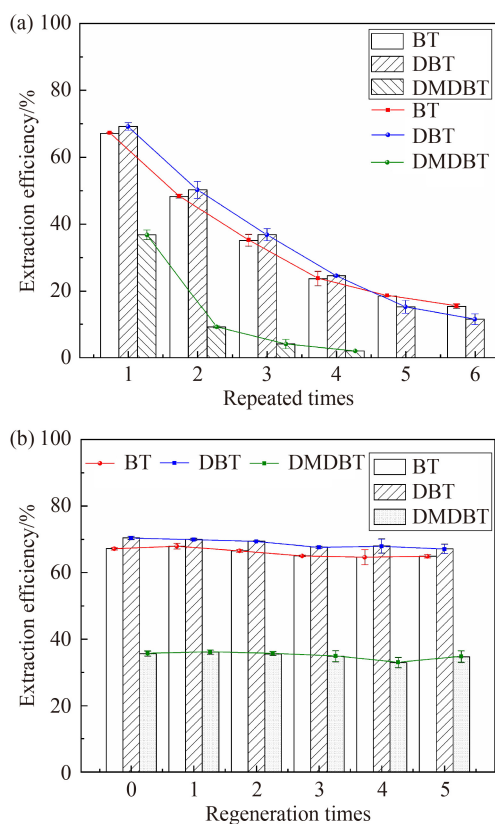


Fig. 9 Effects of (a) recycling and (b) regeneration of IL on desulfurization efficiency.

regenerated [IL][PEG200] was used in the next extraction cycle under the same extraction conditions. Compared with fresh [IL][PEG200], the extraction efficiency of the regenerated reagent remained stable after five cycles, as shown in Fig. 9(b). ^1H NMR and FTIR spectra (Fig. S5, cf. ESM) confirmed that the structure of the regenerated [IL][PEG200] was stable and unchanged.

3.3.6 Possible mechanism

The extraction capacity mainly depends on the interaction between [IL][PEG200] and the sulfides. To explore the mechanism of the extraction process, in-depth research was carried out in conjunction with ^1H NMR, as shown in Fig. 10. Considering that the sulfides were insoluble in [IL][PEG200], the organic phase was tested by ^1H NMR after extraction (room temperature, $v_{[\text{IL}][\text{PEG200}]}:v_{\text{oil}} = 8:1$, 30 min). Where the contents of BT, DBT, and DMDBT were lower, displacement of the corresponding sulfides in the spectrum might be masked; therefore, the interactions could only be judged by the peak shift changes of [IL][PEG200]. For DBT, the active hydrogen signal of [IL][PEG200] in the supernatant after extraction moved from 13.07 ppm to a high field of 13.22 ppm. This effect was mainly attributed to the ring. Combined with the data presented in Section 3.2, the cations in [DBU][L-Pyro] also played a major role.

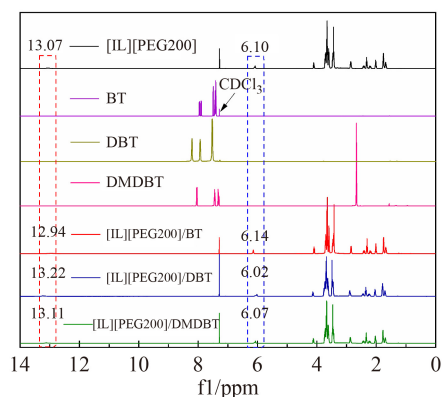


Fig. 10 ^1H NMR (CDCl_3 , 500 MHz) characterization of [IL][PEG200] on EDS.

A comparison between the results obtained between this work and other previously reported results is listed in Table 4. The desulfurization efficiency of sulfur compounds in model oil obtained in this work has significance for reference purposes.

4 Conclusions

[DBU][L-Pyro] IL was synthesized and used for extractive desulfurization. The IL structure was simulated and confirmed by characterization and using Gaussian 09 software. The infrared spectrum obtained by frequency calculation was consistent with the experimental spectrum, which confirmed rationality of the IL structure optimization. The order of single-stage desulfurization selectivity of the IL was DMDBT < BT < DBT. This was verified by the interaction energies between IL and BT, DBT, and DMDBT. The interaction forces were subjected to reduced density gradient analysis to visualize and categorize the non-covalent interactions. This analysis indicated that van der Waals force and hydrogen bonding interaction contributed to the extractive desulfurization. PEG200 was added to reduce the mass-transfer resistance and economic cost. When the extraction conditions were $v_{[\text{IL}][\text{PEG200}]}:v_{\text{oil}} = 1:1$, room temperature, the single-stage BT, DBT, and DMDBT removal efficiencies by [IL][PEG200] were 67.32 (15 min), 70.83 (10 min), and 36.16% (15 min), respectively. Addition of *p*-xylene and cyclohexene to the model oil had little effect and could be ignored. After four cycles, the contents of BT and DBT decrease from 500 ppm to 10 ppm. DMDBT exhibited larger steric hindrance, so the required extraction times were relatively longer. The extractant was stable and effective after multiple regenerations. These results provide new insight on the suitability of IL as an alternative solvent to capture thiophene sulfides from fuel oil.

Acknowledgements This work was supported by the National Natural

Table 4 Comparison of different desulfurization systems

| Extractants | V _{ext} :V _{oil} | T/°C | S-contents/ppm | Model oil | Extraction cycle | Sulfur removal/% | Ref. |
|--|------------------------------------|------------------|----------------|--------------------|------------------|------------------|-----------|
| TEA:BA | 1.5:1 | 30 | 500 | <i>n</i> -Octane | 1 | 70.61 (BT) | [35] |
| TEA:2OHBA | 1.5:1 | 30 | 500 | <i>n</i> -Octane | 1 | 81.0 (DBT) | [35] |
| TBAB:HCOOH | 1:0.5 | 30 | 500 | <i>n</i> -Octane | 1 | 80.47 (DBT) | [11] |
| TBAC:2MA | 1:1 | 30 | 1000 | <i>n</i> -Octane | 5 | 99.2 (BT) | [36] |
| [C ₄ mpip]FeCl ₄ | 1 g:5 mL | 45 | 500 | Tetradecane | 5 | 96 | [37] |
| ChCl:2CH ₃ COOH | 1:5 | 30 | 500 | – | 1 | 7.8 (DBT) | [38] |
| [C ₂ (Mim) ₂](H ₂ SO ₄) ₂ | 1:1 (w:w) | 30 | – | FCC | 1 | 56.9 | [22] |
| TBAB/2EG | 1.2:1 | 25 | 500 | Isooctane | 1 | 81.2 (DBT) | [39] |
| [DBU][Im] | 1:1 | room temperature | 500 | <i>n</i> -Octane | 1 | 79.2 (DBT) | [25] |
| [Epy][NTf ₂] | 1:1 (w:w) | 25 | 500 | <i>n</i> -Octane | 1 | 43.94 (BT) | [40] |
| [Bpy][NTf ₂] | 1:1 (w:w) | 25 | 500 | <i>n</i> -Octane | 1 | 58.50 (BT) | [40] |
| [Hpy][NTf ₂] | 1:1 (w:w) | 25 | 500 | <i>n</i> -Octane | 1 | 63.86 (BT) | [40] |
| [TMG][Im] | 1:1 | room temperature | 500 | <i>n</i> -Octane | 1 | 69.4 (DBT) | [25] |
| TBAB:FA | 1:1 | 30 | 500 | | 1 | 60 (DBT) | [41] |
| | | | | | | 72.68 (TH) | [23] |
| TDA:SA | 1:1 (w:w) | 25 | 500 | <i>n</i> -Dodecane | 5 | 76.31 (BT) | [23] |
| | | | | | | 83.94 (DBT) | [23] |
| [IL][PEG200] | 1:1 | 20 | 500 | Tetradecane | 4 | 98.8 (BT/DBT) | This work |

Science Foundation of China (Grant Nos. 22125802, 22078010 and U1862113) and the Big Science Project from BUCT (Grant No. XK180301).

Electronic Supplementary Material Supplementary material is available in the online version of this article at <https://dx.doi.org/10.1007/s11705-022-2167-x> and is accessible for authorized users.

References

- Majid M F, Zaid H F M, Kait C F, Jumbri K, Yuan L C, Rajasuriyan S. Futuristic advance and perspective of deep eutectic solvent for extractive desulfurization of fuel oil: a review. *Journal of Molecular Liquids*, 2020, 306: 112870
- Yu G J, Wu X J, Wei L, Zhou Z Y, Liu W, Zhang F, Qu Y X, Ren Z Q. Desulfurization of diesel fuel by one-pot method with morpholinium-based Brønsted acidic ionic liquid. *Fuel*, 2021, 296: 120551
- Jiang W, Dong L, Liu W, Guo T, Li H P, Yin S, Zhu W S, Li H M. Biodegradable choline-like deep eutectic solvents for extractive desulfurization of fuel. *Chemical Engineering and Processing*, 2017, 115: 34–38
- Hao L W, Wang M R, Shan W J, Deng C L, Ren W Z, Shi Z Z, Lü H Y. L-Proline-based deep eutectic solvents (DESS) for deep catalytic oxidative desulfurization (ODS) of diesel. *Journal of Hazardous Materials*, 2017, 339: 216–222
- Zhu Z G, Lu H Y, Zhang M, Yang H Q. Deep eutectic solvents as non-traditionally multifunctional media for the desulfurization process of fuel oil. *Physical Chemistry Chemical Physics*, 2021, 23(2): 785–805
- Liu J, Li W Y, Feng J, Gao X. Effects of Fe species on promoting the dibenzothiophene hydrodesulfurization over the Pt/gamma-Al₂O₃ catalysts. *Catalysis Today*, 2021, 371: 247–257
- Chen L G, Xu Y, Wang B H, Yun J, Dehghani F, Xie Y T, Liang X. Mg-modified CoMo/Al₂O₃ with enhanced catalytic activity for the hydrodesulfurization of 4,6-dimethyldibenzothiophene. *Catalysis Communications*, 2021, 155: 106316
- Rezaee M, Feyzi F, Dehghani M R. Extractive desulfurization of dibenzothiophene from normal octane using deep eutectic solvents as extracting agent. *Journal of Molecular Liquids*, 2021, 333: 115991
- Lima F, Gouvenaux J, Branco L C, Silvestre A J D, Marrucho I M. Towards a sulfur clean fuel: deep extraction of thiophene and dibenzothiophene using polyethylene glycol-based deep eutectic solvents. *Fuel*, 2018, 234: 414–421
- Almashjary K H, Khalid M, Dharaskar S, Jagadish P, Walvekar R, Gupta T C S M. Optimisation of extractive desulfurization using choline chloride-based deep eutectic solvents. *Fuel*, 2018, 234: 1388–1400
- Li J J, Xiao H, Tang X D, Zhou M. Green carboxylic acid-based deep eutectic solvents as solvents for extractive desulfurization. *Energy & Fuels*, 2016, 30(7): 5411–5418
- Ali S H, Hamad D M, Albusairi B H, Fahim M A. Removal of dibenzothiophenes from fuels by oxy-desulfurization. *Energy & Fuels*, 2009, 23(12): 5986–5994
- Welton T. Ionic liquids in catalysis. *Coordination Chemistry Reviews*, 2004, 248(21–24): 2459–2477
- Player L C, Chan B, Lui M Y, Masters A F, Maschmeyer T. Toward an understanding of the forces behind extractive desulfurization of fuels with ionic liquids. *ACS Sustainable Chemistry & Engineering*, 2019, 7(4): 4087–4093
- Camargo D, Andrade R S, Ferreira G A, Mazzer H, Cardozo L, Iglesias M. Investigation of the rheological properties of protic ionic liquids. *Journal of Physical Organic Chemistry*, 2016, 29(11): 604–612
- Paucar N E, Kiggins P, Blad B, De Jesus K, Afrin F, Pashikanti S, Sharma K. Ionic liquids for the removal of sulfur and nitrogen compounds in fuels: a review. *Environmental Chemistry Letters*, 2021, 19(2): 1205–1228
- Abro R, Abdeltawab A A, Al-Deyab S S, Yu G R, Qazi A B, Gao S R, Chen X C. A review of extractive desulfurization of fuel oils using ionic liquids. *RSC Advances*, 2014, 4(67): 35302–35317

18. Holbrey J D, Lo'pez-Martin I, Rothenberg G, Seddon K R, Silvero G, Zheng X. Desulfurisation of oils using ionic liquids: selection of cationic and anionic components to enhance extraction efficiency. *Green Chemistry*, 2008, 10(1): 87–92
19. Butt H S, Lethesh K C, Fiksdahl A. Fuel oil desulfurization with dual functionalized imidazolium based ionic liquids. *Separation and Purification Technology*, 2020, 248: 116959
20. Raj J J, Magaret S, Pranesh M, Lethesh K C, Devi W C, Mutalib M A. Dual functionalized imidazolium ionic liquids as a green solvent for extractive desulfurization of fuel oil: toxicology and mechanistic studies. *Journal of Cleaner Production*, 2019, 213: 989–998
21. Ibrahim M H, Hayyan M, Hashim M A, Hayyan A. The role of ionic liquids in desulfurization of fuels: a review. *Renewable & Sustainable Energy Reviews*, 2017, 76: 1534–1549
22. Li J J, Lei X J, Tang X D, Zhang X P, Wang Z Y, Jiao S. Acid dicationic ionic liquids as extractants for extractive desulfurization. *Energy & Fuels*, 2019, 33(5): 4079–4088
23. Wang Q, Zhang T, Zhang S L, Fan Y C, Chen B. Extractive desulfurization of fuels using trialkylamine-based protic ionic liquids. *Separation and Purification Technology*, 2020, 231: 115923
24. Butt H S, Lethesh K C, Fiksdahl A. Fuel oil desulfurization with dual functionalized imidazolium based ionic liquids. *Separation and Purification Technology*, 2020, 248: 116959
25. Li M X, Zhou Z Y, Zhang F, Chai W S, Zhang L L, Ren Z Q. Deep oxidative-extractive desulfurization of fuels using benzyl-based ionic liquid. *AIChE Journal*. American Institute of Chemical Engineers, 2016, 62(11): 4023–4034
26. Ren Z Q, Wei L, Zhou Z Y, Zhang F, Liu W. Extractive desulfurization of model oil with protic ionic liquids. *Energy & Fuels*, 2018, 32(9): 9172–9181
27. Ahmed O U, Mjalli F S, Talal A W, Al-Wahaibi Y, Nashef I M. Extractive desulfurization of liquid fuel using modified pyrrolidinium and phosphonium based ionic liquid solvents. *Journal of Solution Chemistry*, 2018, 47(3): 468–483
28. Wang J L, Zhao R J, Han B X, Tang N, Li K X. Extractive and oxidative desulfurization of model oil in polyethylene glycol. *RSC Advances*, 2016, 6(41): 35071–35075
29. Jiang W, Zhu K, Li H P, Zhu L H, Hua M Q, Xiao J, Wang C, Yang Z Z, Chen G Y, Zhu W S, Li H, Dai S. Synergistic effect of dual Brønsted acidic deep eutectic solvents for oxidative desulfurization of diesel fuel. *Chemical Engineering Journal*, 2020, 394: 124831
30. Alecu I M, Zheng J J, Zhao Y, Truhlar D G. Computational thermochemistry: scale factor databases and scale factors for vibrational frequencies obtained from electronic model chemistries. *Journal of Chemical Theory and Computation*, 2010, 6(9): 2872–2887
31. Wang X, Jiang W, Zhu W S, Li H P, Yin S, Chang Y H, Li H M. A simple and cost-effective extractive desulfurization process with novel deep eutectic solvents. *RSC Advances*, 2016, 6(36): 30345–30352
32. Lu T, Chen F W. Multiwfn: a multifunctional wavefunction analyzer. *Journal of Computational Chemistry*, 2012, 33(5): 580–592
33. Wagle D V, Deakyn C A, Baker G A. Quantum chemical insight into the interactions and thermodynamics present in choline chloride based deep eutectic solvents. *Journal of Physical Chemistry B*, 2016, 120(27): 6739–6746
34. Jiang W, Li H, Wang C, Liu W, Guo T, Liu H, Zhu W S, Li H M. Synthesis of ionic liquid-based deep eutectic solvents for extractive desulfurization of fuel. *Energy & Fuels*, 2016, 30(10): 8164–8170
35. Zhao X, Zhu G, Jiao L, Yu F, Xie C. Formation and extractive desulfurization mechanisms of aromatic acid based deep eutectic solvents: an experimental and theoretical study. *Chemistry*, 2018, 24(43): 11021–11032
36. Shu C, Sun T. Extractive desulfurisation of gasoline with tetrabutyl ammonium chloride-based deep eutectic solvents. *Separation and Purification Technology*, 2016, 51(8): 1336–1343
37. Jiang W, Zhu W, Li H, Xin W, Sheng Y, Chang Y, Li H M. Temperature-responsive ionic liquid extraction and separation of the aromatic sulfur compounds. *Fuel*, 2015, 140: 590–596
38. Zhu W, Wang C, Li H, Wu P, Xun S, Jiang W, Chen Z G, Zhao Z, Li H M. One-pot extraction combined with metal-free photochemical aerobic oxidative desulfurization in deep eutectic solvent. *Green Chemistry*, 2015, 17(4): 2464–2472
39. Khan N, Srivastava V C. Quaternary ammonium salts-based deep eutectic solvents: utilization in extractive desulfurization. *Energy & Fuels*, 2021, 35(15): 12734–12745
40. Wu J M, Wu X M, Zhao P P, Wang Z H, Zhang L Z, Xu D M, Gao J. Extraction desulphurization of fuels using ZIF-8-based porous liquid. *Fuel*, 2021, 300: 121013
41. Makos P, Boczkaj G. Deep eutectic solvents based highly efficient extractive desulfurization of fuels-eco-friendly approach. *Journal of Molecular Liquids*, 2019, 296: 111916